

Stress reduction in sputter deposited films using nanostructured compliant layers by high working-gas pressures

Tansel Karabacak,^{a)} Jay. J. Senkevich, Gwo-Ching Wang, and Toh-Ming Lu
*Department of Physics, Applied Physics, and Astronomy, Rensselaer Polytechnic Institute, Troy,
New York 12180-3590*

(Received 1 October 2004; accepted 13 December 2004; published 27 June 2005)

We present a strategy of stress reduction in sputter deposited films by a nano-compliant layer at the substrate using physically self-assembled nanostructures obtained at high working-gas pressures prior to the deposition of a continuous film. This technique is all *in situ*, and the nanostructures are made of the same material as the deposited thin film and requires no lithography process. This nanostructured layer has a lower material density and can act as a compliant layer to reduce the stress of the subsequently deposited continuous film grown under low gas pressure. By using this approach we were able to reduce stress values significantly in sputter deposited tungsten films and the strategy of alternating high and low Ar gas pressures leads to the growth of much thicker films without delamination. © 2005 American Vacuum Society. [DOI: 10.1116/1.1861940]

I. INTRODUCTION

The control of stress in physical vapor deposited thin films is of continued interest due to its close relationship to technologically important material properties. Further, thin film stress often determines its adhesive strength to the substrate,¹⁻³ the limit of film thickness without cracking, buckling, or delamination,⁴⁻⁹ electrical properties,¹⁰⁻¹² and optical properties such as distortions in x-ray masks.¹³

It has been shown^{14,15} that the intrinsic stress in sputtered tungsten films is correlated to Thornton's structure zone model (SZM).¹⁶ The SZM relates the microstructures of sputtered thin films to the most prominent deposition parameters such as working-gas pressure and substrate temperature. The studies by Haghiri-Gosnet *et al.*¹⁴ and Windischmann¹⁵ have revealed that the transition from zone 1 of a porous and columnar structure to zone T of a denser film, e.g., by passing from high to lower working-gas pressures, corresponded to a dramatic change of stress from high tensile to high compressive values (i.e., from a few GPa tensile to a few GPa compressive for tungsten). The rapid change of stress with pressure allows only a narrow window of pressures that yields reasonably low-stress values (i.e., \leq a few hundred MPa for tungsten). Therefore, obtaining low-stress films by controlling the working-gas pressure (at a fixed pressure during deposition) has been difficult and is not a robust method.¹⁴ In the high-pressure part of zone 1 it is possible to produce low-stress films. However, these films exhibit poor electrical properties due to the columnar microstructure. This is partially due to adsorbed oxygen in the voids, which results in an increase of stress to compressive.¹⁴

Similarly, the stress is a sensitive function of dc bias voltage¹¹ and substrate temperature^{14,17} near the transition between tensile and compressive values, which makes the stress control difficult. A rf-substrate biasing technique has been shown to improve the stress control over an optimum

regime of cathode current, pressure, and the rf-substrate bias values.¹¹ On the other hand, the method is sensitive to the type of materials to be deposited, and finding the optimum parameter space can be challenging. In addition, Maier *et al.* studied the effect of plasma-etch surface treatment of graphite substrates before a deposition on the adhesion properties of tungsten films sputter deposited at various temperatures.⁹ Their plasma treatment is a chemical method that suffers limitations of the type of substrate materials and the material to be deposited. Also, the deposition may need high substrate temperatures. Recently, Windt¹⁸ was able to reduce the stress in sputter deposited W films using a bilayer structure of W/Cr. He adjusted the deposition conditions to give compressive and tensile stress in W and Cr layers, respectively. His results suggest that with a suitable choice of layer thicknesses for W and Cr, the net stress in the bilayer can be made to balance each other.

An approach by Karabacak *et al.*¹⁹ demonstrated that a thin layer of nanostructures formed by an oblique angle deposition technique can act as a compliant layer and effectively reduces the stress of the continuous film atop. The use of a compliant layer in stress reduction has been shown to be a more robust technique compared to other approaches mentioned above. During oblique angle deposition, the incident flux that approaches on a tilted substrate is preferentially deposited on the higher surface heights due to the shadowing effect. This physical self-assembly process results in the formation of nanorods. By this method, the nanostructured compliant layer (NCL) of low material density is obtained *in situ* and the nanostructures are made of the same material as the deposited thin film. This method does not require any lithography steps.

In this article we present another, and maybe a simpler way, of obtaining a NCL. We suggest that nanostructures of a NCL can also be produced using the SZM of sputter deposited films themselves. A "revised SZM" study by Messier, Giri, and Roy²⁰ has shown that zone 1 of classical SZM in fact consists of five different subzones of columnar "nano-

^{a)}Author to whom correspondence should be addressed; electronic mail: karab@rpi.edu

structures” with typical sizes varying from 1 to 3 nm to 200–400 nm. At high working-gas pressures, enhanced collision and scattering events result in particles that obliquely incident on the substrate surface. Therefore, the shadowing effects give rise to the formation of columnar structures. The reduced ion bombardment at high pressures slows down the adatom mobility and therefore results in less dense films. The nanocolumns are typically separated from each other by voids that are lower density regions.²¹ This indicates that the low-density regions can be as small as atomic scales, and also at the same time be as large as a few tens of nanometers in size. Even in the deposition conditions that normally favor the formation of dense films, thin film strain that built up during the growth may lead to the formation of columnar structures. Huang *et al.* observed that sputtered Cu can form alternating layers of $\langle 111 \rangle$ and $\langle 110 \rangle$ texture where it is in the form of denser and columnar structure, respectively.²² They explain their result by a self-organization mechanism that includes shadowing effect and competition between the strain and surface energies.

Once forming the NCL using a high working-gas pressure, we can decrease the working gas pressure *in situ* to deposit the usual continuous dense layer of material. We can expect that the compliant layer will relieve the stress in the continuous thin film, which then results in better adhesion, larger critical thickness, and better quality films. The process can be repeated to form thick multilayer films.

II. EXPERIMENT

In order to experiment with the approach described above, we used a dc magnetron sputtering system to deposit tungsten films. W films were deposited on oxidized *p*-Si(100) (resistivity 12–25 Ω cm) wafers (diameter ~ 7.6 cm) using a 99.95% pure W cathode (diameter ~ 7.6 cm). The substrates were mounted on the sample holder located at a distance of about 15 cm from the cathode. The base pressure of $\sim 2 \times 10^{-6}$ Torr was achieved by a turbo-molecular pump backed by a mechanical pump. In all the deposition experiments, the power was 200 W. We used an ultrapure Ar flow to generate the plasma.

In a previous study by Shen *et al.*, who used a similar W deposition system, it has been shown that the film stress gets close to zero at around ~ 15 mTorr.²³ Therefore, we set the Ar pressure to 15.0 mTorr to obtain the low-stress NCL of columnar W. For the low-pressure value, we used 2.0 mTorr which would give dense but stressed films. We performed W depositions on silicon wafers starting from the high-pressure step and successively changing the pressure between high to low at the end of each layer. The thicknesses of the films were determined by a step profilometer and also verified by scanning electron microscopy (SEM) cross-sectional images. The deposition rates were measured to be ~ 12.0 and ~ 16.5 nm/min at the Ar pressures of 2.0 and 15.0 mTorr, respectively. In this study, we set the thicknesses of the NCL and the denser film to 165 and 120 nm, respectively. In addition, we will label the very first NCL layer on the silicon substrate as $n=1$, the second denser W layer as $n=2$, the

following NCL as $n=3$, and so on. The surface topography was investigated using optical microscopy and atomic force microscopy (AFM). We used a contact-mode AFM (Park Scientific Auto CP) where the radius of the silicon tip used was about 10 nm, and the side angle was about 12° . The scan sizes were $2 \times 2 \mu\text{m}^2$ with 512×512 pixels. The root mean square (rms) roughness values were extracted from the quantitative surface height values. The crystal structure information was studied by x-ray diffraction (XRD) measurements using a Scintag diffractometer with a Cu target ($\lambda = 1.5405 \text{ \AA}$) operated at 50 kV and 30 mA. The diffractometer was calibrated with respect to the peak positions of a Si calibration standard.

The measurements of intrinsic thin film stress were performed by using a dual wavelength ($\lambda_1=670$ nm and $\lambda_2=750$ nm) Flexus 2320 system, which uses a wafer curvature technique. The film stress σ then was calculated using Stoney’s equation²⁴

$$\sigma = \frac{1}{6R} \frac{E}{(1-\nu)} \frac{d_{\text{sub}}^2}{d}, \quad (1)$$

where E , ν , and d_{sub} are Young’s modulus, Poisson’s ratio, and thickness of the substrate, respectively, and d is the film thickness (assuming $d \ll d_{\text{sub}}$). Before a deposition, the R is the radius of curvature of the reference wafer (R_1). After a deposition, the R becomes the relative substrate radius of curvature and is calculated as $R=R_1R_2/(R_1-R_2)$, where R_1 and R_2 are the radii of curvatures before and after depositions, respectively. In conventional notation, positive signs of film stress correspond to tensile and negative signs to compressive stress values. However, since all the tungsten films we investigated were in compressive stress state, in this article positive signs will be used to represent the compressive stress.

Qualitative adhesion tests were made by using a scotch tape peel test. However, in cases where the film was already peeling off or flaking by itself, we did not perform the peel test and considered this film as failing in adhesion.

III. RESULTS AND DISCUSSION

With no compliant layer present, we observed that the W film starts to delaminate and peels off after thickness ~ 240 nm. Figures 1(a)–1(c) show optical microscopy topographies of the delaminated W film at various thicknesses. The delamination patterns are in the form of randomly oriented wrinkles at thickness ~ 240 nm [Fig. 1(a)]; parallel periodic wrinkles at ~ 600 nm [Fig. 1(b)], and irregular-shaped flakes at ~ 1440 nm [Fig. 1(c)]. The whole film shown in Fig. 1(a) and the light-gray regions in Figs. 1(b) and 1(c) were the buckled films that delaminated but still loosely adhered to the substrate. The dark-gray regions in Figs. 1(b) and 1(c) were exposed Si surfaces after the film peeled off completely at those places. Some portions of the W film that were peeled off but still barely attached to the adhering film from their edges were shown as the black regions in Fig. 1(b). Similar decohesion patterns for W films were observed before^{5,6} and explained by the high compressive

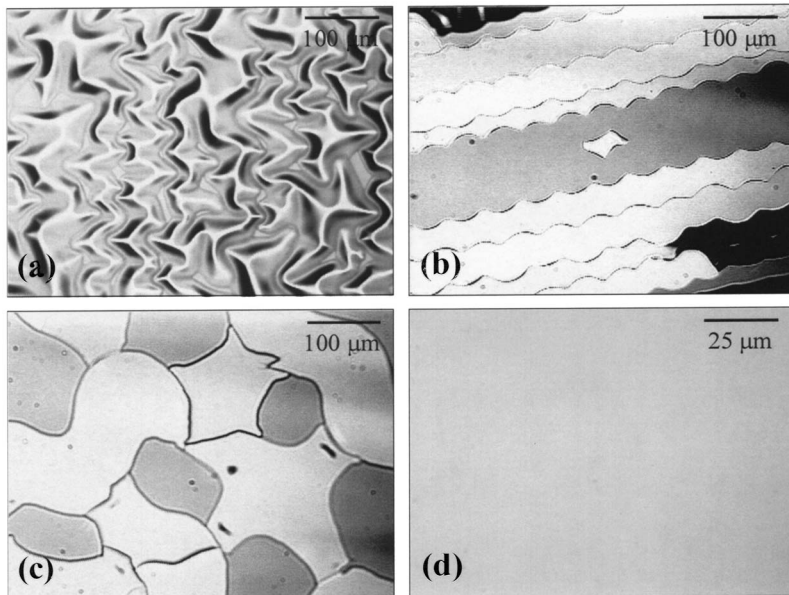


FIG. 1. Optical microscopy images of tungsten morphologies: (a) ~ 240 nm, (b) ~ 600 nm, (c) ~ 1440 -nm-thick W films deposited on bare Si substrates. Film delaminations can be seen clearly. Black color regions in (b) are the W film that delaminated and completely peeled off. Light-gray parts in (b) and (c) are delaminated W films that still barely stick to the Si surface, and dark-gray regions are exposed Si surface areas. (d) A ~ 570 -nm-thick multilayer W film obtained by successively depositing the W film at high/low Ar pressures (four individual and successive layers of ~ 165 nm at 15 mTorr and ~ 120 nm at 2 mTorr). The film is smooth ($\text{rms} = 1.3 \pm 0.1$ nm) and has a good adhesion. The scale bars are $100 \mu\text{m}$ for (a), (b), and (c) and $25 \mu\text{m}$ for (d).

sive stress values in the film and followed by relaxation in the form of wrinkles. As a driving force of the wrinkle formation, the elastic energy that originates from the film stress stored in the layer/substrate system is considered.^{6,25} Gille and Rau²⁵ suggested that at sufficiently high stress values, the poorly bonded areas and heterogeneities in the film may induce elastic instabilities similar to the well-known “Euler instability of a loaded column.” These instabilities can cause periodic delaminations or buckling patterns if the release rate of the elastic energy is equal to the debonding surface energy. In cases where instabilities are biaxial and have different wavelengths at the orthogonal directions the delamination pattern can be in the form of wavy wrinkles similar to the ones in Fig. 1(b). However, at lower stress values below a critical limit the wrinkles cannot propagate and they become randomly oriented as in Fig. 1(a). On the other hand, if the film stress passes a higher limit, the growth of wrinkles can become unstable and the film can delaminate as a whole or in the form of flakes such as in Fig. 1(c). In addition, O’Keefe and Stutz observed that high compressive stress values of sputter deposited W films decreased as a function of time while the film relaxed and delaminated in the form of wrinkles.⁵

In contrast, the multilayer NCL/dense W films of high/low Ar pressure (e.g., 15 mTorr/2 mTorr) did not delaminate for any of the thicknesses we investigated (e.g., up to ~ 2300 nm formed by $n=16$ individual layers). Figure 1(d) compares a smooth ~ 570 -nm-thick multilayer W film ($\text{rms} = 1.3 \pm 0.1$ nm, $n=4$) to Figs. 1(a)–1(c) of delaminated W films at various thicknesses with no compliant layer. In addition, all these W films deposited with NCL passed the scotch tape peel test that indicates the enhancement in adhesion.

Figure 2 shows the measured stress values of single layer low Ar pressure (no compliant layer) and multilayer (high/low Ar pressure) tungsten films as a function of total film thickness. Single layer W films made under low Ar pressure

quickly develop very high compressive stress values (~ 2.35 GPa) even at ~ 120 nm thickness. On the other hand, a single layer of high-pressure W film made by using an NCL step (~ 165 nm thick) has a low stress value ~ 0.05 GPa (off scale and is not shown in Fig. 2). This is consistent with the previous studies on the change of stress with the working-gas pressure.^{14,15} The maximum temperature of the substrate during the deposition was measured to be $\sim 85^\circ\text{C}$. It has been previously shown that a $\sim 50^\circ\text{C}$ increase in substrate temperature during sputter deposition of tungsten corresponded to a negligible “thermally induced” stress value of ~ 50 MPa.¹⁰ Therefore, in our samples the stress values are mostly incorporated during film growth or “growth induced” stress.

The multilayer structures formed by these individual layers of high/low pressure have mild stress values (e.g.,

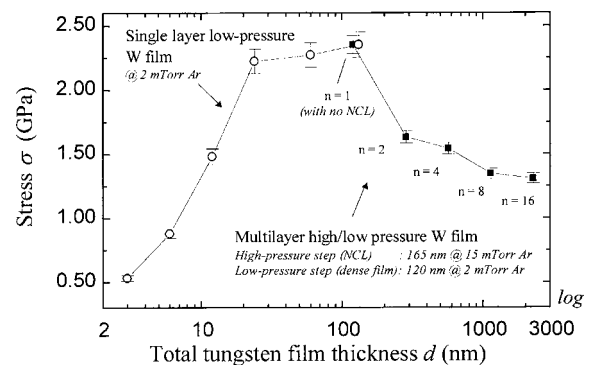


FIG. 2. Measured stress values (compressive) of single layer low Ar pressure (open circles) and multilayer high/low Ar pressure tungsten films (filled squares) are plotted as a function of total film thickness in a semilog scale. A multilayer structure starts first with a high-pressure step on the Si wafer. However, the first data point corresponds to a ~ 120 nm W film at low pressure. The “ n ” represents the total number of individual layers. The high-pressure step gives rise to the formation of a nanostructured compliant layer (NCL), while for the low-pressure step we obtained a denser layer with higher stress. All the multilayer films have good adhesion.

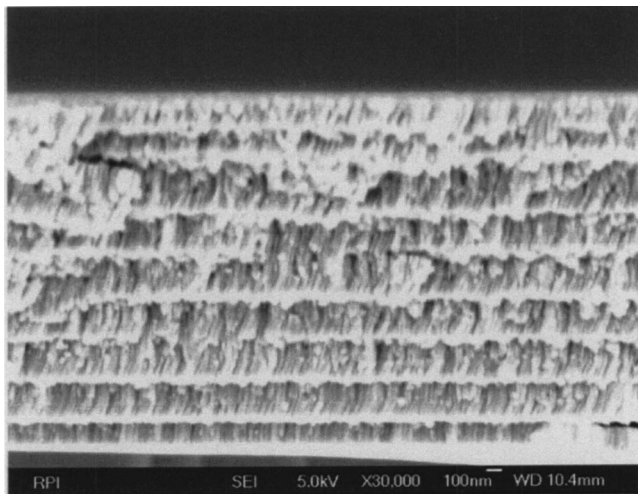


FIG. 3. Cross-sectional SEM image of a multilayer W film obtained by successively depositing the W film *in situ* first at 15 mTorr to obtain the nanostructured compliant layer (NCL) (~ 165 nm, $n=1$) nm, second at 2 mTorr to obtain the denser film (~ 120 nm, $n=2$) nm, and then repeated the NCL/denser film seven more times (total number of individual layers $n=16$). The multilayer film is ~ 2300 nm thick. The scale bar is 100 nm.

~ 1.30 GPa at ~ 2300 nm thickness) as shown in the Fig. 2. Interestingly, unlike the single layer W films made under low pressure, the stress of multilayer film decreases as the total thickness increases. The incorporation of each additional NCL seems to increase the efficiency of compliance in the multilayer film. In addition, the stress seems to level off at higher thicknesses of the multilayer film. This may be due to the competition between the stress buildup with the increase of total film thickness and the relaxation mechanisms associated with the NCLs. At higher thicknesses these two effects can reach an equilibrium state and the stress becomes stabilized. Therefore, NCL used in this way allows us to fabricate very thick films with reasonable low stresses. As an example, Fig. 3 shows an SEM cross-section image of ~ 2300 -nm-thick film, where the multilayer structure can also be realized.

In addition, the crystal structure of W films *with* and *without* NCL and their densities are investigated. Depending on the growth conditions and thicknesses of the films, the sputter deposition of tungsten films can give rise to either the α -phase W, which has the equilibrium bcc structure, or the metastable β -phase W, which has an A15 (cubic) structure, or a mixture of both phases.^{14,26} The lattice constants are 3.16 and 5.04 Å for α -W and β -W, respectively. These two phases may have very different properties, for example, the measured resistivity of β -W film is an order of magnitude higher than that of the α -W film.²⁷ Figure 4 compares the XRD plot of a low-pressure single layer W film of ~ 340 nm (as measured from the nondelaminated region of the wafer) to a multilayer film of high/low pressure of ~ 2300 nm thick. The XRD profiles are very similar for both types of films. The polycrystalline films consist of a mixture of α and β phases. However, the dominant α phase can be realized with the existence of a strong $\alpha(110)$ peak for both the low-pressure and the multilayer high/low-pressure W films.

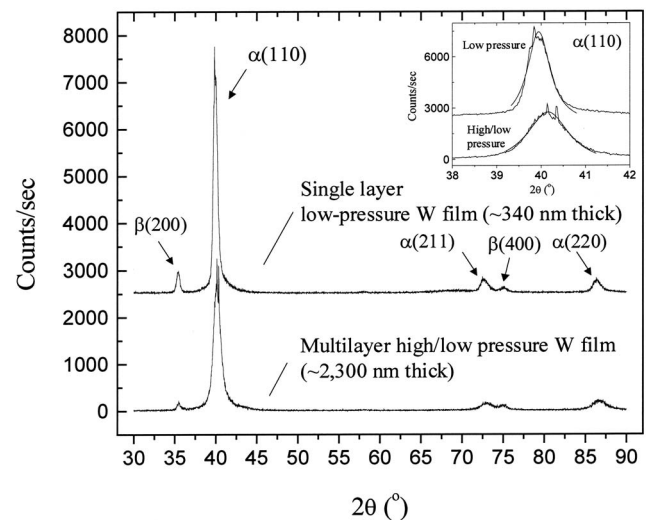


FIG. 4. X-ray diffraction (XRD) spectra of a single layer W film made under low Ar pressure and a multilayer W film made under alternating high/low Ar pressures. The intensity for the single layer W film spectrum in the y axis is offset for clarity. The inset is the zoomed in of $\alpha(110)$ peak profiles. Both the experimental peaks (thick line curves) and the smooth line fits (thin line curves) show the peaks shift towards smaller 2θ values due to a compressive stress in these films.

Moreover, the position of the XRD $\alpha(110)$ peaks shifted towards smaller 2θ angles from the equilibrium position at $2\theta=40.262^\circ$. For example, see the inset in Fig. 4 where the peaks at $\sim 39.945^\circ$ and $\sim 40.159^\circ$ are for a single layer low-pressure and the multilayer high/low-pressure W film, respectively. This type of shift indicates the existence of larger atomic plane spacing, and has been explained to originate from a compressive stress in the film.²⁸ The location of the $\alpha(110)$ peak for the low-pressure W film ($\sim 39.945^\circ$) corresponds to a lattice spacing of ~ 3.189 Å. This is about $\sim 0.79\%$ larger than the equilibrium lattice parameter of an α -W (~ 3.164 Å) film. On the other hand, the $\alpha(110)$ peak for a multilayer W film shows a smaller shift ($\sim 40.159^\circ$) that corresponds to a lattice spacing of ~ 3.172 Å, which is only $\sim 0.25\%$ larger than the equilibrium lattice spacing. This is consistent with the smaller stress values that we observed in our multilayer W films.

IV. CONCLUSION

In conclusion, it has been shown that a nano-compliant layer formed by a high working-gas pressure processing can provide stress reduction, adhesion improvement, and a high critical thickness for sputter deposited W thin films. The technique is all *in situ* and the nanostructures are made of the same material as the deposited thin film. This method does not require any lithography steps. The nanostructure layer has a lower material density and can act as a compliant layer to reduce the stress of the subsequent deposited continuous film. By using this approach we were able to significantly reduce stress values in sputter deposited tungsten films on Si surfaces. These lower stress thin films exhibit stronger adhesions to the substrates thereby avoiding delamination. In ad-

dition, by using a multilayer structure made under alternating high and low gas pressures, we obtained very thick W with high structural integrity.

ACKNOWLEDGMENTS

This work is supported by the NSF. The authors thank D.-X. Ye for taking the scanning electron micrographs of the samples.

- ¹C. Creton and E. Papon, *MRS Bull.* **28**, 419 (2003).
- ²L.-H. Lee, *Fundamentals of Adhesion* (Plenum, New York, 1992), p. 363.
- ³D. L. Smith, *Thin-Film Deposition: Principles and Practice* (McGraw-Hill, New York, 1995), pp. 193–200.
- ⁴K.-D. Lee, E. T. Ogawa, S. Yoon, X. Lu, and P. S. Ho, *Appl. Phys. Lett.* **82**, 2032 (2003).
- ⁵M. J. O'Keefe and S. E. Stutz, *Mater. Res. Soc. Symp. Proc.* **472**, 233 (1997).
- ⁶D. C. Meyer, A. Klingner, Th. Holz, and P. Paufler, *Appl. Phys. A: Mater. Sci. Process.* **69**, 657 (1999).
- ⁷M. D. Kriese and W. W. Gerberich, *J. Mater. Res.* **14**, 3019 (1999).
- ⁸G. Zazzara and I. E. Reimanis, *Surf. Coat. Technol.* **111**, 92 (1999).
- ⁹H. Maier, J. Luthin, M. Balden, J. Linke, F. Koch, and H. Bolt, *Surf. Coat. Technol.* **142–144**, 733 (2001).
- ¹⁰T. J. Vink, W. Walrave, J. L. C. Daams, A. G. Dirks, M. A. J. Somers, and K. J. A. van den Aker, *J. Appl. Phys.* **74**, 988 (1993).
- ¹¹A. Bensaoula, J. C. Wolfe, A. Ignatiev, F.-O. Fong, and T.-S. Leung, *J. Vac. Sci. Technol. A* **2**, 389 (1984).
- ¹²D. S. Gardner and P. A. Flinn, *J. Appl. Phys.* **67**, 1831 (1990).
- ¹³R. R. Kola, G. K. Celler, J. Frackowiak, C. W. Jurgensen, and L. E. Trimble, *J. Vac. Sci. Technol. B* **9**, 3301 (1991).
- ¹⁴A. M. Haghiri-Gosnet, F. R. Ladan, C. Mayeux, H. Launois, and M. C. Joncour, *J. Vac. Sci. Technol. A* **7**, 2663 (1989).
- ¹⁵H. Windischmann, *J. Vac. Sci. Technol. A* **9**, 2431 (1991).
- ¹⁶J. A. Thornton, *J. Vac. Sci. Technol.* **11**, 666 (1974); **12**, 830 (1975); J. A. Thornton, *Annu. Rev. Mater. Sci.* **7**, 239 (1977); *J. Vac. Sci. Technol. A* **4**, 3059 (1986); *Proc. SPIE* **821**, 95 (1987).
- ¹⁷R. Rastogi, V. Dharmadhikari, and A. Diebold, *J. Vac. Sci. Technol. A* **9**, 2453 (1991).
- ¹⁸D. L. Windt, *J. Vac. Sci. Technol. B* **17**, 1385 (1999).
- ¹⁹T. Karabacak, C. R. Picu, J. J. Senkevich, G.-C. Wang, and T.-M. Lu, *J. Appl. Phys.* **96**, 5740 (2004).
- ²⁰R. Messier, A. P. Giri, and R. A. Roy, *J. Vac. Sci. Technol. A* **2**, 500 (1984).
- ²¹H. S. Witham, P. Chindaudom, I. An, R. W. Collins, R. Messier, and K. Vedam, *J. Vac. Sci. Technol. A* **11**, 1881 (1993).
- ²²H. Huang, H. L. Wei, C. H. Woo, and X. X. Zhang, *Appl. Phys. Lett.* **82**, 4265 (2003).
- ²³Y. G. Shen, Y. W. Mai, Q. C. Zhang, D. R. McKenzie, W. D. McFall, and W. E. McBride, *J. Appl. Phys.* **87**, 177 (2000).
- ²⁴G. C. Stoney, *Proc. R. Soc. London, Ser. A* **32**, 172 (1909).
- ²⁵G. Gille and B. Rau, *Thin Solid Films* **120**, 109 (1984).
- ²⁶T. Karabacak, A. Mallikarjunan, J. P. Singh, D. Ye, G.-C. Wang, and T.-M. Lu, *Appl. Phys. Lett.* **83**, 3096 (2003).
- ²⁷K. Y. Ahn, *Thin Solid Films* **153**, 469 (1987).
- ²⁸I. C. Noyan, T. M. Shaw, and C. C. Goldsmith, *J. Appl. Phys.* **82**, 4300 (1997).